

## Article

# Abundant Wave Accurate Analytical Solutions of the Fractional Nonlinear Hirota–Satsuma–Shallow Water Wave Equation

Chen Yue <sup>1,†</sup>, Dianchen Lu <sup>1,†</sup> and Mostafa M. A. Khater <sup>1,2,\*</sup>

<sup>1</sup> Department of Mathematics, Faculty of Science, Jiangsu University, Zhenjiang 212013, China; 2111802001@stmail.ujs.edu.cn (C.Y.); dclu@ujs.edu.cn (D.L.)

<sup>2</sup> Department of Mathematics, Obour High Institute for Engineering and Technology, Cairo 11828, Egypt

\* Correspondence: 1000005364@ujs.edu.cn

† The authors did all this work equally.

**Abstract:** This research paper targets the fractional Hirota’s analytical solutions–Satsuma ( $\mathcal{HS}$ ) equations. The conformable fractional derivative is employed to convert the fractional system into a system with an integer–order. The extended simplest equation (ESE) and modified Kudryashov (MKud) methods are used to construct novel solutions of the considered model. The solutions’ accuracy is investigated by handling the computational solutions with the Adomian decomposition method. The solutions are explained in some different sketches to demonstrate more novel properties of the considered model.

**Keywords:** fractional hirota–satsuma equation; analytical solutions; semi–analytical simulation



**Citation:** Yue, C.; Lu, D.; Khater, M.M.A. Abundant Wave Accurate Analytical Solutions of the Fractional Nonlinear Hirota–Satsuma–Shallow Water Wave Equation. *Fluids* **2021**, *6*, 235. <https://doi.org/10.3390/fluids6070235>

Academic Editor: Amparo López Jiménez

Received: 5 March 2021

Accepted: 4 April 2021

Published: 29 June 2021

**Publisher’s Note:** MDPI stays neutral with regard to jurisdictional claims in published maps and institutional affiliations.



**Copyright:** © 2021 by the author. Licensee MDPI, Basel, Switzerland. This article is an open access article distributed under the terms and conditions of the Creative Commons Attribution (CC BY) license (<https://creativecommons.org/licenses/by/4.0/>).

## 1. Introduction

Recently, the integrable nonlinear partial differential equations (INLPDEs) have been used in many typical applications [1–3]. These applications depend on the solitary wave solutions’ features, which are considered a fundamental tool for discovering more properties of the formulated phenomena by INLPDEs [4–7]. These solutions are handled to investigate the elastic and inelastic interaction in waves’ pulse through the transmission [8–11]. Studying these solutions has attracted the focus of much research, forcing them to formulate many analytical techniques for obtaining this kind of wave that gives them to investigate more properties of these solutions [12–14]. Such techniques are used to construct the analytical solutions for example extended tanh–expansion method, rational–expansion method, sine–Gordon expansion method, inverse Scattering transformation, Darbous transformation, Riccati, expansion method, multiple exp-function method, etc. [13,15–26].

In this article, we study a well-known model in INLPDEs presented by Hirota et al. [27–29]. This model is known by  $\mathcal{HS}$  shallow water wave equation which is given by

$$\left\{ \begin{array}{l} \mathcal{D}_\tau^\varrho \mathfrak{E} = \mathcal{D}_\tau^\varrho \mathfrak{E}_{\Xi\Xi} + 3 \mathfrak{E} \mathcal{D}_\tau^\varrho \mathfrak{E} - 3 \mathfrak{E}_\Xi \mathcal{D}_\tau^\varrho \mathcal{E} + \mathfrak{E}_\Xi, \\ \mathfrak{E}_\Xi = -\mathfrak{E}. \end{array} \right. \quad (1)$$

where  $\mathfrak{E} = \mathfrak{E}(\Xi, \tau)$ ,  $\mathcal{E} = \mathcal{E}(\Xi, \tau)$ ,  $0 < \varrho \leq 1$ . System (1) describes the dynamical behavior of the solitary wave in the shallow water. Applying the next wave transformation  $[\mathcal{E} = \mathcal{S}(\Gamma), \mathfrak{E} = \mathfrak{S}(\Gamma), \Gamma = \Xi + \lambda \frac{t^\varrho}{\varrho}]$  where  $\lambda$  is an arbitrary constant, then substituting the second equation in the system into the first, convert the above–fractional system into the following equation with an-integer order

$$-\lambda \mathfrak{S}'' - 3\lambda \mathfrak{S}^2 + (\lambda - 1) \mathfrak{S} = 0. \quad (2)$$

Handling Equation (2) by the homogeneous balance principles and the following auxiliary equation method of ESE and MKud method  $\left[ f'(\Gamma) = h_3 f(\Gamma)^2 + h_2 f(\Gamma) + h_1 \& Q'(\Gamma) = \log(a) (Q(\Gamma)^2 - Q(\Gamma)) \right]$ , gets the value of balance equal two. Consequently, the general solutions of Equation (2) are given by

$$\mathfrak{S}(\Gamma) = \left\{ a_2 f(\Gamma)^2 + a_1 f(\Gamma) + \frac{a_{-2}}{f(\Gamma)^2} + \frac{a_{-1}}{f(\Gamma)} + a_0, a_2 Q(\Gamma)^2 + a_1 Q(\Gamma) + a_0 \right\} \quad (3)$$

where  $a_{-2}, a_{-1}, a_0, a_1, a_2$  are arbitrary constants to be calculated later.

The rest sections are ordered as follows, we test, by means of two suggested analytical techniques [30–32], the analytical solutions to the nonlinear  $\mathcal{HS}$  fractional equation. We search for the accuracy of the solutions we obtain in conjunction with the semi-analytical AD schema [33,34] in Section 2 part. In Section 3 we clarify the innovation of our approach and its physical interpretation. In the Section 4 portion, the outcome of a paper is summed up.

## 2. Computational Solutions vs. Accuracy

Here, we employ two recent analytical schemes (ESE and MKud methods) to formulate some novel computational wave solutions of the considered model. Additionally, the evaluated solutions are used to calculate the initial and boundary conditions. These conditions allow applying the AD method to test the accuracy of the obtained solutions and used schemes. This investigation takes the following steps:

### 2.1. Analytical Solutions

Applying the ESE and MKud methods' framework gets the values of the above-mentioned parameters as following:

1. *Through the ESE method's steps gets the next values:*  
**Set I**

$$a_{-2} \rightarrow 0, a_{-1} \rightarrow 0, a_0 \rightarrow \frac{1}{3}(-h_2^2 - 2h_1h_3), a_1 \rightarrow -2h_2h_3, a_2 \rightarrow -2h_3^2, \lambda \rightarrow \frac{1}{h_2^2 - 4h_1h_3 + 1}.$$

### Set II

$$a_{-2} \rightarrow -2h_1^2, a_{-1} \rightarrow -2h_1h_2, a_0 \rightarrow \frac{1}{3}(-h_2^2 - 2h_1h_3), a_1 \rightarrow 0, a_2 \rightarrow 0, \lambda \rightarrow \frac{1}{h_2^2 - 4h_1h_3 + 1}.$$

### Set III

$$a_{-2} \rightarrow 0, a_{-1} \rightarrow 0, a_0 \rightarrow -2h_1h_3, a_1 \rightarrow -2h_2h_3, a_2 \rightarrow -2h_3^2, \lambda \rightarrow \frac{1}{-h_2^2 + 4h_1h_3 + 1}.$$

### Set IV

$$a_{-2} \rightarrow -2h_1^2, a_{-1} \rightarrow -2h_1h_2, a_0 \rightarrow -2h_1h_3, a_1 \rightarrow 0, a_2 \rightarrow 0, \lambda \rightarrow \frac{1}{-h_2^2 + 4h_1h_3 + 1}.$$

Consequently, the exact solutions of the fractional nonlinear  $\mathcal{HS}$  equation are constructed in the following. For  $h_2 = 0, h_1h_3 > 0$ , we find

$$\mathfrak{E}_{I,1}(\Xi, \tau) = \frac{1}{3}(-2)h_1h_3 \left( 3 \tan^2 \left( \sqrt{h_1h_3} \left( \frac{\tau^\varrho}{(1-4h_1h_3)\varrho} + \Xi + \vartheta \right) \right) + 1 \right), \quad (4)$$

$$\mathfrak{E}_{I,2}(\Xi, \tau) = \frac{1}{3}(-2)h_1h_3 \left( 3 \cot^2 \left( \sqrt{h_1h_3} \left( \frac{\tau^\varrho}{(1-4h_1h_3)\varrho} + \Xi + \vartheta \right) \right) + 1 \right), \quad (5)$$

$$\mathfrak{E}_{\text{II},1}(\Xi, \tau) = \frac{1}{3}(-2)h_1h_3 \left( 3 \cot^2 \left( \sqrt{h_1h_3} \left( \frac{\tau^\varrho}{(1-4h_1h_3)\varrho} + \Xi + \vartheta \right) \right) + 1 \right), \quad (6)$$

$$\mathfrak{E}_{\text{II},2}(\Xi, \tau) = \frac{1}{3}(-2)h_1h_3 \left( 3 \tan^2 \left( \sqrt{h_1h_3} \left( \frac{\tau^\varrho}{(1-4h_1h_3)\varrho} + \Xi + \vartheta \right) \right) + 1 \right), \quad (7)$$

$$\mathfrak{E}_{\text{III},1}(\Xi, \tau) = -2h_1h_3 \sec^2 \left( \sqrt{h_1h_3} \left( \frac{\tau^\varrho}{(1-4h_1h_3)\varrho} + \Xi + \vartheta \right) \right), \quad (8)$$

$$\mathfrak{E}_{\text{III},2}(\Xi, \tau) = -2h_1h_3 \csc^2 \left( \sqrt{h_1h_3} \left( \frac{\tau^\varrho}{(1-4h_1h_3)\varrho} + \Xi + \vartheta \right) \right), \quad (9)$$

$$\mathfrak{E}_{\text{IV},1}(\Xi, \tau) = -2h_1h_3 \csc^2 \left( \sqrt{h_1h_3} \left( \frac{\tau^\varrho}{(1-4h_1h_3)\varrho} + \Xi + \vartheta \right) \right), \quad (10)$$

$$\mathfrak{E}_{\text{IV},2}(\Xi, \tau) = -2h_1h_3 \sec^2 \left( \sqrt{h_1h_3} \left( \frac{\tau^\varrho}{(1-4h_1h_3)\varrho} + \Xi + \vartheta \right) \right). \quad (11)$$

For  $h_2 = 0$ ,  $h_1h_3 < 0$ , we find

$$\mathfrak{E}_{\text{I},3}(\Xi, \tau) = \frac{2}{3}h_1h_3 \left( 3 \tanh^2 \left( \sqrt{-h_1h_3} \left( \frac{\tau^\varrho}{(1-4h_1h_3)\varrho} + \Xi \right) \mp \frac{\log(\vartheta)}{2} \right) - 1 \right), \quad (12)$$

$$\mathfrak{E}_{\text{I},4}(\Xi, \tau) = \frac{2}{3}h_1h_3 \left( 3 \operatorname{csch}^2 \left( \sqrt{-h_1h_3} \left( \frac{\tau^\varrho}{(1-4h_1h_3)\varrho} + \Xi \right) \mp \frac{\log(\vartheta)}{2} \right) + 2 \right), \quad (13)$$

$$\mathfrak{E}_{\text{II},3}(\Xi, \tau) = \frac{2}{3}h_1h_3 \left( 3 \operatorname{csch}^2 \left( \sqrt{-h_1h_3} \left( \frac{\tau^\varrho}{(1-4h_1h_3)\varrho} + \Xi \right) \mp \frac{\log(\vartheta)}{2} \right) + 2 \right), \quad (14)$$

$$\mathfrak{E}_{\text{II},4}(\Xi, \tau) = \frac{2}{3}h_1h_3 \left( 3 \tanh^2 \left( \sqrt{-h_1h_3} \left( \frac{\tau^\varrho}{(1-4h_1h_3)\varrho} + \Xi \right) \mp \frac{\log(\vartheta)}{2} \right) - 1 \right), \quad (15)$$

$$\mathfrak{E}_{\text{III},3}(\Xi, \tau) = -2h_1h_3 \operatorname{sech}^2 \left( \sqrt{-h_1h_3} \left( \frac{\tau^\varrho}{(1-4h_1h_3)\varrho} + \Xi \right) \mp \frac{\log(\vartheta)}{2} \right), \quad (16)$$

$$\mathfrak{E}_{\text{III},4}(\Xi, \tau) = 2h_1h_3 \operatorname{csch}^2 \left( \sqrt{-h_1h_3} \left( \frac{\tau^\varrho}{(1-4h_1h_3)\varrho} + \Xi \right) \mp \frac{\log(\vartheta)}{2} \right), \quad (17)$$

$$\mathfrak{E}_{\text{IV},3}(\Xi, \tau) = 2h_1h_3 \operatorname{csch}^2 \left( \sqrt{-h_1h_3} \left( \frac{\tau^\varrho}{(1-4h_1h_3)\varrho} + \Xi \right) \mp \frac{\log(\vartheta)}{2} \right), \quad (18)$$

$$\mathfrak{E}_{\text{IV},4}(\Xi, \tau) = -2h_1h_3 \operatorname{sech}^2 \left( \sqrt{-h_1h_3} \left( \frac{\tau^\varrho}{(1-4h_1h_3)\varrho} + \Xi \right) \mp \frac{\log(\vartheta)}{2} \right). \quad (19)$$

For  $h_1 = 0$ ,  $h_2 > 0$ , we find

$$\mathfrak{E}_{I,5}(\Xi, \tau) = h_2^2 \left( -\frac{2}{\left( h_3 e^{h_2 \left( \frac{\tau^\varrho}{(h_2^2+1)\varrho} + \Xi + \vartheta \right)} - 1 \right)^2} - \frac{2}{h_3 e^{h_2 \left( \frac{\tau^\varrho}{(h_2^2+1)\varrho} + \Xi + \vartheta \right)} - 1} - \frac{1}{3} \right), \quad (20)$$

$$\mathfrak{E}_{III,5}(\Xi, \tau) = -\frac{2h_2^2 h_3 e^{h_2 \left( \frac{\tau^\varrho}{(h_2^2+1)\varrho} + \Xi + \vartheta \right)}}{\left( h_3 e^{h_2 \left( \frac{\tau^\varrho}{(h_2^2+1)\varrho} + \Xi + \vartheta \right)} - 1 \right)^2}. \quad (21)$$

For  $h_1 = 0, h_2 < 0$ , we find

$$\mathfrak{E}_{I,6}(\Xi, \tau) = \frac{1}{3} \left( -\frac{6h_3^4 e^{2h_2 \left( \frac{\tau^\varrho}{(h_2^2+1)\varrho} + \Xi + \vartheta \right)}}{\left( h_3 e^{h_2 \left( \frac{\tau^\varrho}{(h_2^2+1)\varrho} + \Xi + \vartheta \right)} + 1 \right)^2} + 6h_2 h_3 \left( 1 - \frac{1}{h_3 e^{h_2 \left( \frac{\tau^\varrho}{(h_2^2+1)\varrho} + \Xi + \vartheta \right)} + 1} \right) - h_2^2 \right), \quad (22)$$

$$\mathfrak{E}_{III,6}(\Xi, \tau) = 2h_3 \left( h_3 \left( -\frac{1}{h_3 e^{h_2 \left( \frac{\tau^\varrho}{(h_2^2+1)\varrho} + \Xi + \vartheta \right)} + 1} - 1 \right) - \frac{h_2 - 2h_3}{h_3 e^{h_2 \left( \frac{\tau^\varrho}{(h_2^2+1)\varrho} + \Xi + \vartheta \right)} + 1} + h_2 \right). \quad (23)$$

For  $4h_1 h_3 > h_2^2$ , we find

$$\mathfrak{E}_{I,7}(\Xi, \tau) = \frac{1}{6} \left( h_2^2 - 4h_1 h_3 \right) \left( 3 \sec^2 \left( \frac{1}{2} \sqrt{4h_1 h_3 - h_2^2} \left( \frac{\tau^\varrho}{(h_2^2 - 4h_1 h_3 + 1)\varrho} + \Xi + \vartheta \right) \right) - 2 \right), \quad (24)$$

$$\mathfrak{E}_{I,8}(\Xi, \tau) = \frac{1}{6} \left( h_2^2 - 4h_1 h_3 \right) \left( 3 \csc^2 \left( \frac{1}{2} \sqrt{4h_1 h_3 - h_2^2} \left( \frac{\tau^\varrho}{(h_2^2 - 4h_1 h_3 + 1)\varrho} + \Xi + \vartheta \right) \right) - 2 \right), \quad (25)$$

$$\begin{aligned} \mathfrak{E}_{II,5}(\Xi, \tau) = & -\frac{h_2^2}{3} + \frac{4h_1 h_3 h_2}{h_2 - \sqrt{4h_1 h_3 - h_2^2} \tan \left( \frac{1}{2} \sqrt{4h_1 h_3 - h_2^2} \left( \frac{\tau^\varrho}{(h_2^2 - 4h_1 h_3 + 1)\varrho} + \Xi + \vartheta \right) \right)} \\ & + \frac{2}{3} h_1 h_3 \left( -\frac{12h_1 h_3}{\left( h_2 - \sqrt{4h_1 h_3 - h_2^2} \tan \left( \frac{1}{2} \sqrt{4h_1 h_3 - h_2^2} \left( \frac{\tau^\varrho}{(h_2^2 - 4h_1 h_3 + 1)\varrho} + \Xi + \vartheta \right) \right) \right)^2} - 1 \right), \end{aligned} \quad (26)$$

$$\begin{aligned} \mathfrak{E}_{\text{II},6}(\Xi, \tau) = & -\frac{h_2^2}{3} + \frac{4h_1h_3h_2}{h_2 - \sqrt{4h_1h_3 - h_2^2} \cot\left(\frac{1}{2}\sqrt{4h_1h_3 - h_2^2}\left(\frac{\tau^\varrho}{(h_2^2 - 4h_1h_3 + 1)\varrho} + \Xi + \vartheta\right)\right)} \\ & + \frac{2}{3}h_1h_3\left(-\frac{12h_1h_3}{\left(h_2 - \sqrt{4h_1h_3 - h_2^2} \cot\left(\frac{1}{2}\sqrt{4h_1h_3 - h_2^2}\left(\frac{\tau^\varrho}{(h_2^2 - 4h_1h_3 + 1)\varrho} + \Xi + \vartheta\right)\right)\right)^2} - 1\right), \end{aligned} \quad (27)$$

$$\mathfrak{E}_{\text{III},7}(\Xi, \tau) = \frac{h_2^2 - 4h_1h_3}{\cos\left(\sqrt{4h_1h_3 - h_2^2}\left(\frac{\tau^\varrho}{(h_2^2 - 4h_1h_3 + 1)\varrho} + \Xi + \vartheta\right)\right) + 1}, \quad (28)$$

$$\mathfrak{E}_{\text{III},8}(\Xi, \tau) = \frac{1}{2}\left(h_2^2 - 4h_1h_3\right) \csc^2\left(\frac{1}{2}\sqrt{4h_1h_3 - h_2^2}\left(\frac{\tau^\varrho}{(h_2^2 - 4h_1h_3 + 1)\varrho} + \Xi + \vartheta\right)\right), \quad (29)$$

$$\begin{aligned} \mathfrak{E}_{\text{IV},5}(\Xi, \tau) = & 2h_1h_3\left(h_2^2 - 4h_1h_3\right) \Bigg/ \left(\left(h_2 \cos\left(\frac{1}{2}\sqrt{4h_1h_3 - h_2^2}\left(\frac{\tau^\varrho}{(h_2^2 - 4h_1h_3 + 1)\varrho} + \Xi + \vartheta\right)\right)\right.\right. \\ & \left.\left.- \sqrt{4h_1h_3 - h_2^2} \sin\left(\frac{1}{2}\sqrt{4h_1h_3 - h_2^2}\left(\frac{\tau^\varrho}{(h_2^2 - 4h_1h_3 + 1)\varrho} + \Xi + \vartheta\right)\right)\right)^2, \end{aligned} \quad (30)$$

$$\begin{aligned} \mathfrak{E}_{\text{IV},6}(\Xi, \tau) = & 2h_1h_3\left(h_2^2 - 4h_1h_3\right) \Bigg/ \left(h_2 \sin\left(\frac{1}{2}\sqrt{4h_1h_3 - h_2^2}\left(\frac{\tau^\varrho}{(h_2^2 - 4h_1h_3 + 1)\varrho} + \Xi + \vartheta\right)\right)\right. \\ & \left.- \sqrt{4h_1h_3 - h_2^2} \cos\left(\frac{1}{2}\sqrt{4h_1h_3 - h_2^2}\left(\frac{\tau^\varrho}{(h_2^2 - 4h_1h_3 + 1)\varrho} + \Xi + \vartheta\right)\right)\right)^2. \end{aligned} \quad (31)$$

2. Through the MKud method's steps gets the next values  
**Set I**

$$a_0 \rightarrow 0, a_1 \rightarrow 2\log^2(a), a_2 \rightarrow -2\log^2(a), \lambda \rightarrow \frac{1}{1 - \log^2(a)}.$$

**Set II**

$$a_0 \rightarrow -\frac{1}{3}\log^2(a), a_1 \rightarrow 2\log^2(a), a_2 \rightarrow -2\log^2(a), \lambda \rightarrow \frac{1}{\log^2(a) + 1}.$$

Consequently, the exact solutions of the fractional nonlinear  $\mathcal{HS}$  equation are constructed in the following

$$\mathfrak{E}_I(\Xi, \tau) = \frac{2\log^2(a)\left(\left(1 \pm a^{\frac{\tau^\varrho}{\varrho - \varrho\log^2(a)} + \Xi}\right) - 1\right)}{\left(1 \pm a^{\frac{\tau^\varrho}{\varrho - \varrho\log^2(a)} + \Xi}\right)^2}, \quad (32)$$

$$\mathfrak{E}_{\text{II}}(\Xi, \tau) = \frac{1}{3}\log^2(a)\left(\frac{6\left(\left(1 \pm a^{\frac{\tau^\varrho}{\varrho\log^2(a) + \varrho} + \Xi}\right) - 1\right)}{\left(1 \pm a^{\frac{\tau^\varrho}{\varrho\log^2(a) + \varrho} + \Xi}\right)^2} - 1\right). \quad (33)$$

## 2.2. Solutions' Accuracy

Checking the accuracy of the obtained exact solutions of the  $\mathcal{HSI}$  equation along with ESE and MKud methods with respect to Equations (12) and (32) for  $\left[ h_1 = -1, h_3 = 1, h_2 = 0 \& a = 3 \right]$ , gets the following semi-analytical solutions;

$$\mathfrak{E}_0|_{\mathfrak{E}_{1,3}}(\Xi) = \frac{2}{3}, \quad (34)$$

$$\mathfrak{E}_0|_{\mathfrak{E}_I}(\Xi) = \frac{\log^2(3)}{2}, \quad (35)$$

$$\mathfrak{E}_1|_{\mathfrak{E}_{1,3}}(\Xi) = -2\Xi^2, \quad (36)$$

$$\mathfrak{E}_1|_{\mathfrak{E}_I}(\Xi) = -\frac{1}{8}\Xi^2 \log^4(3) - \frac{1}{4}\Xi^2 \log^2(3) + \frac{\Xi^2 \log^2(3)}{4(1 - \log^2(3))} - \frac{\Xi^2 \log^4(3)}{4(1 - \log^2(3))}, \quad (37)$$

$$\mathfrak{E}_2|_{\mathfrak{E}_{1,3}}(\Xi) = \frac{4\Xi^4}{3}, \quad (38)$$

$$\mathfrak{E}_2|_{\mathfrak{E}_I}(\Xi) = \frac{1}{48}\Xi^4 \log^6(3) + \frac{1}{96}\Xi^4 \log^4(3) + \frac{\Xi^4 \log^6(3)}{96(1 - \log^2(3))} - \frac{\Xi^4 \log^4(3)}{96(1 - \log^2(3))}, \quad (39)$$

$$\mathfrak{E}_3|_{\mathfrak{E}_{1,3}}(\Xi) = \frac{2\Xi^4}{3} - \frac{26\Xi^6}{45}, \quad (40)$$

$$\mathfrak{E}_3|_{\mathfrak{E}_I}(\Xi) = -\frac{\Xi^6 \log^8(3)}{1152} - \frac{\Xi^6 \log^6(3)}{1440} - \frac{\Xi^6 \log^8(3)}{1440(1 - \log^2(3))} + \frac{\Xi^6 \log^6(3)}{1440(1 - \log^2(3))} + \frac{1}{32}\Xi^4 \log^6(3). \quad (41)$$

Consequently, the semi-analytical solutions are given by

$$\mathfrak{E}_{\text{appro}}|_{\mathfrak{E}_{1,3}}(\Xi) = -\frac{26\Xi^6}{45} + 2\Xi^4 - 2\Xi^2 + \frac{2}{3}, \quad (42)$$

$$\begin{aligned} \mathfrak{E}_{\text{appro}}|_{\mathfrak{E}_I}(\Xi) = & -\frac{\Xi^6 \log^8(3)}{1152} - \frac{\Xi^6 \log^6(3)}{1440} - \frac{\Xi^6 \log^8(3)}{1440(1 - \log^2(3))} + \frac{\Xi^6 \log^6(3)}{1440(1 - \log^2(3))} + \frac{5}{96}\Xi^4 \log^6(3) \\ & + \frac{1}{96}\Xi^4 \log^4(3) + \frac{\Xi^4 \log^6(3)}{96(1 - \log^2(3))} - \frac{\Xi^4 \log^4(3)}{96(1 - \log^2(3))} - \frac{1}{8}\Xi^2 \log^4(3) - \frac{1}{4}\Xi^2 \log^2(3) \\ & + \frac{\Xi^2 \log^2(3)}{4(1 - \log^2(3))} - \frac{\Xi^2 \log^4(3)}{4(1 - \log^2(3))} + \frac{\log^2(3)}{2}. \end{aligned} \quad (43)$$

Calculating the exact, semi-analytical solutions based on Equations (42) and (43) gets the following value in Tables 1 and 2:

**Table 1.** Accuracy of the ESE method's solutions through AD method.

Value of $\Xi$	$\xi_{L3}$	$\xi_{\text{appro}} \Big _{\xi_{L3}} (\Xi)$	Absolute Error	Value of $\Xi$	$\xi_{L3}$	$\xi_{\text{appro}} \Big _{\xi_{L3}} (\Xi)$	Absolute Error
0	0.666666667	0.666666667	0	0.26	0.537334231	0.540427702	0.003093471
0.01	0.66646668	0.666466687	$6.66684 \times 10^{-9}$	0.27	0.527670559	0.531271644	0.003601085
0.02	0.66586688	0.665866987	$1.06678 \times 10^{-7}$	0.28	0.517712301	0.521881361	0.00416906
0.03	0.664867746	0.664868286	$5.40129 \times 10^{-7}$	0.29	0.507466562	0.512268611	0.004802049
0.04	0.663470077	0.663471784	$1.70739 \times 10^{-6}$	0.3	0.49694059	0.502445467	0.005504876
0.05	0.661674988	0.661679158	$4.16943 \times 10^{-6}$	0.31	0.486141768	0.492424307	0.006282539
0.06	0.659483911	0.65949256	$8.64823 \times 10^{-6}$	0.32	0.475077598	0.482217803	0.007140204
0.07	0.656898591	0.656914619	$1.60274 \times 10^{-5}$	0.33	0.463755696	0.471838905	0.008083209
0.08	0.653921083	0.653948435	$2.73526 \times 10^{-5}$	0.34	0.452183778	0.461300833	0.009117055
0.09	0.650553747	0.65059758	$4.38328 \times 10^{-5}$	0.35	0.440369653	0.450617058	0.010247405
0.1	0.646799248	0.646866089	$6.68405 \times 10^{-5}$	0.36	0.428321208	0.43980129	0.011480082
0.11	0.64266055	0.642758463	$9.79132 \times 10^{-5}$	0.37	0.416046402	0.428867467	0.012821065
0.12	0.638140907	0.638279661	0.000138754	0.38	0.403553253	0.417829735	0.014276482
0.13	0.633243865	0.633435098	0.000191233	0.39	0.390849829	0.406702435	0.015852606
0.14	0.627973249	0.628230636	0.000257388	0.4	0.377944239	0.395500089	0.01755585
0.15	0.62233316	0.622672585	0.000339425	0.41	0.36484462	0.384237382	0.019392762
0.16	0.616327971	0.616767693	0.000439722	0.42	0.351559131	0.372929146	0.021370015
0.17	0.609962313	0.610523141	0.000560827	0.43	0.33809594	0.361590344	0.023494403
0.18	0.603241075	0.603946535	0.00070546	0.44	0.324463218	0.35023605	0.025772832
0.19	0.596169391	0.597045905	0.000876514	0.45	0.310669125	0.338881435	0.02821231
0.2	0.588752633	0.589829689	0.001077056	0.46	0.296721809	0.327541748	0.03081994
0.21	0.580996403	0.582306733	0.00131033	0.47	0.282629388	0.316232296	0.033602908
0.22	0.572906525	0.574486278	0.001579754	0.48	0.268399947	0.304968423	0.036568476
0.23	0.564489035	0.566377955	0.00188892	0.49	0.254041531	0.293765499	0.039723967
0.24	0.555750171	0.557991772	0.002241601	0.5	0.239562133	0.282638889	0.043076756
0.25	0.546696364	0.549338108	0.002641743	0.51	0.224969687	0.271603943	0.046634256

**Table 2.** Accuracy of the MKud method's solutions through AD method.

Value of $\Xi$	$\xi_I$	$\xi_{\text{appro}} \Big _{\xi_I} (\Xi)$	Absolute Error	Value of $\Xi$	$\xi_I$	$\xi_{\text{appro}} \Big _{\xi_I} (\Xi)$	Absolute Error
0	0.603474	0.603474	0	0.26	0.591331	0.591583	0.000252
0.01	0.603456	0.603456	$5.49 \times 10^{-10}$	0.27	0.590392	0.590686	0.000294
0.02	0.603402	0.603402	$8.79 \times 10^{-9}$	0.28	0.589421	0.589761	0.00034
0.03	0.603311	0.603311	$4.45 \times 10^{-8}$	0.29	0.588416	0.588807	0.000391
0.04	0.603183	0.603183	$1.41 \times 10^{-7}$	0.3	0.587379	0.587827	0.000448
0.05	0.603019	0.60302	$3.43 \times 10^{-7}$	0.31	0.586308	0.58682	0.000511
0.06	0.602819	0.60282	$7.12 \times 10^{-7}$	0.32	0.585206	0.585787	0.000581
0.07	0.602583	0.602584	$1.32 \times 10^{-6}$	0.33	0.584071	0.584728	0.000657
0.08	0.602311	0.602313	$2.25 \times 10^{-6}$	0.34	0.582905	0.583646	0.000741
0.09	0.602002	0.602006	$3.61 \times 10^{-6}$	0.35	0.581707	0.582539	0.000832
0.1	0.601657	0.601663	$5.5 \times 10^{-6}$	0.36	0.580477	0.58141	0.000932
0.11	0.601277	0.601285	$8.05 \times 10^{-6}$	0.37	0.579217	0.580258	0.001041
0.12	0.60086	0.600871	$1.14 \times 10^{-5}$	0.38	0.577926	0.579084	0.001159
0.13	0.600408	0.600423	$1.57 \times 10^{-5}$	0.39	0.576604	0.57789	0.001286
0.14	0.59992	0.599941	$2.11 \times 10^{-5}$	0.4	0.575253	0.576677	0.001424
0.15	0.599396	0.599424	$2.79 \times 10^{-5}$	0.41	0.573871	0.575444	0.001573
0.16	0.598837	0.598873	$3.61 \times 10^{-5}$	0.42	0.57246	0.574193	0.001733
0.17	0.598243	0.598288	$4.6 \times 10^{-5}$	0.43	0.57102	0.572925	0.001905
0.25	0.592235	0.592451	0.000216	0.51	0.558485	0.562275	0.00379

**Table 2.** Cont.

Value of $\Xi$	$\epsilon_I$	$\epsilon_{\text{appro}} _{\epsilon_I}(\Xi)$	Absolute Error	Value of $\Xi$	$\epsilon_I$	$\epsilon_{\text{appro}} _{\epsilon_I}(\Xi)$	Absolute Error
0.18	0.597613	0.597671	$5.78 \times 10^{-5}$	0.44	0.569551	0.571641	0.00209
0.19	0.596948	0.59702	$7.18 \times 10^{-5}$	0.45	0.568053	0.570341	0.002288
0.2	0.596249	0.596337	$8.82 \times 10^{-5}$	0.46	0.566527	0.569027	0.0025
0.21	0.595515	0.595622	0.000107	0.47	0.564973	0.567699	0.002726
0.22	0.594746	0.594876	0.000129	0.48	0.563391	0.566359	0.002968
0.23	0.593943	0.594098	0.000154	0.49	0.561783	0.565008	0.003225
0.24	0.593106	0.59329	0.000183	0.5	0.560147	0.563646	0.003499
0.25	0.592235	0.592451	0.000216	0.51	0.558485	0.562275	0.00379

### 3. Results' Explanation

This paper has constructed some novel solutions of the fractional  $\mathcal{HSI}$  equation by implementing ESE and MKud methods. These solutions have been represented through some different forms (Figures 1–4) in three-dimension, density and spherical plot three-dimensional to illustrate more novel properties of the considered model. Comparing our results with that obtained in [35] which has applied the Hirota bilinear method and symbolic computation on the integer-order of the same model, explains our results' novelty where all our solutions are entirely different from their obtained solutions. Additionally, employing the AD method explains our solutions' accuracy, where the analytical and semi-analytical solutions are almost matching. This matching has been cleared along with Tables 1 and 2 and Figures 5 and 6. Still, it also shows the superiority of the MKud method's solution over the ESE method, as shown in Figure 7.

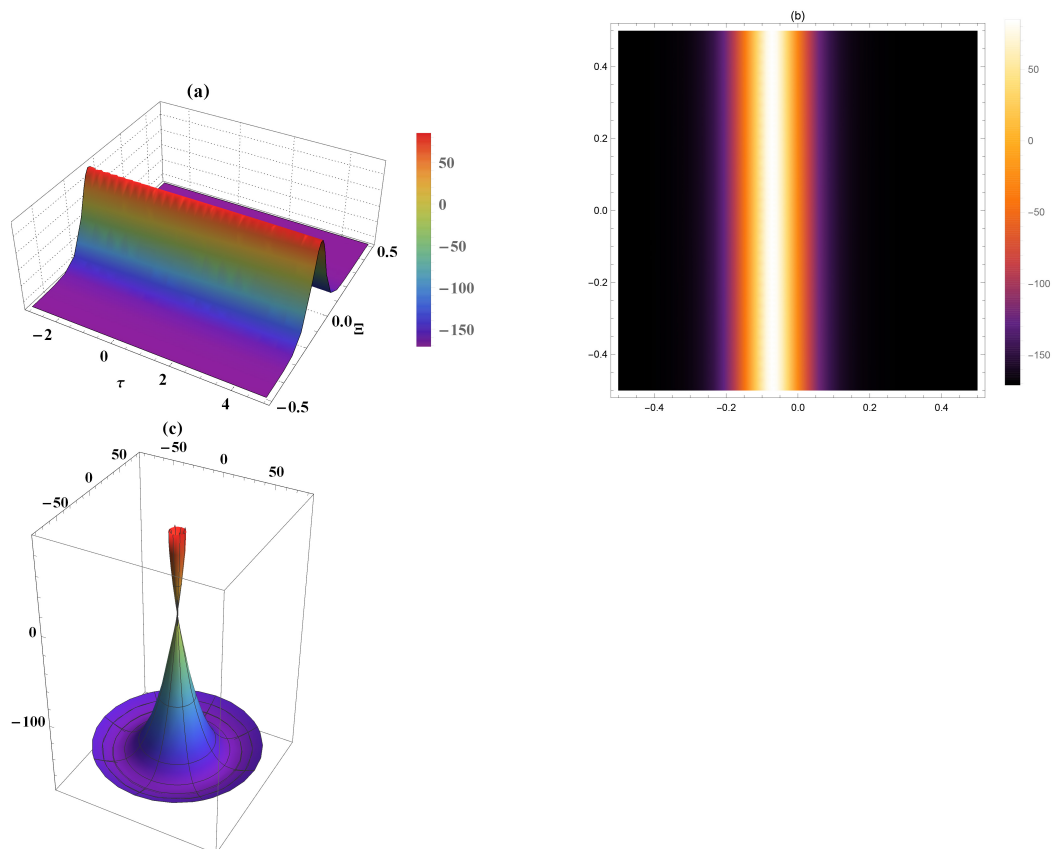


**Figure 1.** Bright solitary wave solution of Equation (12) in (a) three-dimension, (b) density and (c) spherical plot three-dimensional for  $h_1 = -4$ ,  $h_3 = 32$ ,  $\vartheta = 5$ ,  $q = 1$ .

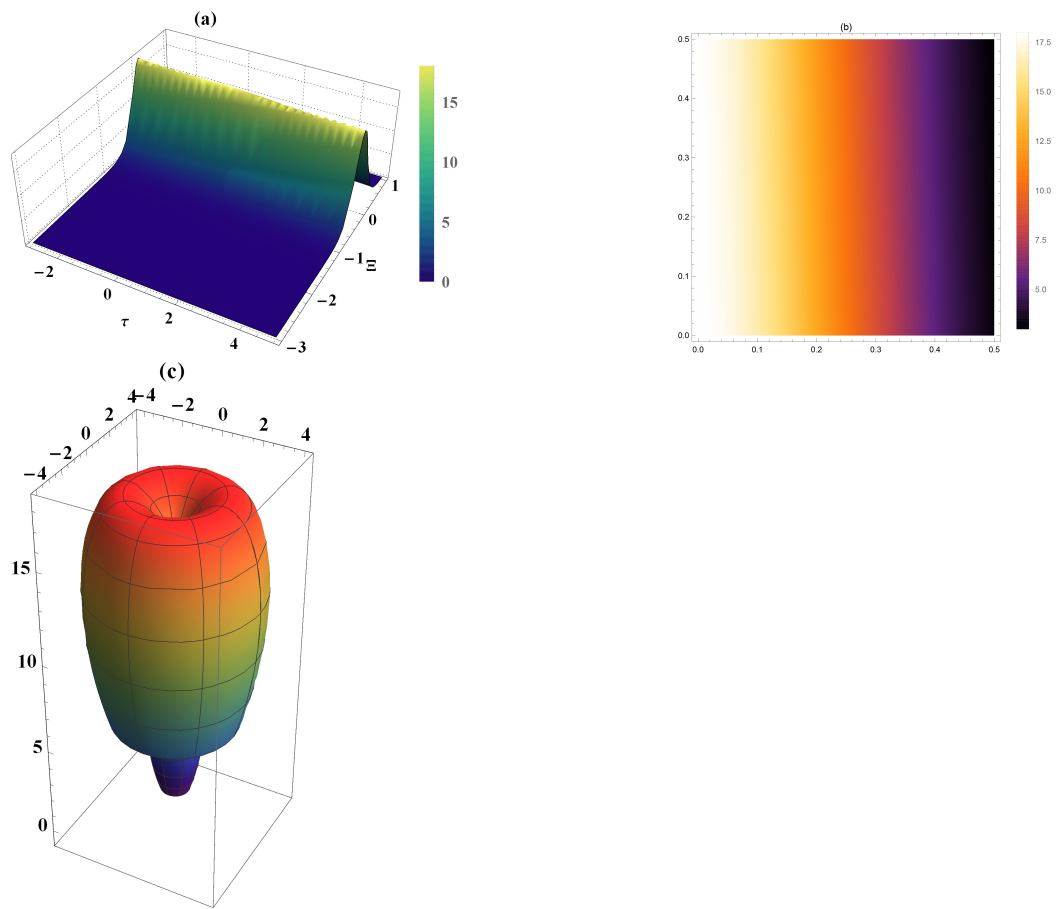


**Figure 2.** Solitary wave solution of Equation (16) in (a) three–dimension, (b) density and (c) spherical plot three–dimensional for  $h_1 = -1$ ,  $h_3 = 9$ ,  $\vartheta = 1$ ,  $\varrho = 1$ .

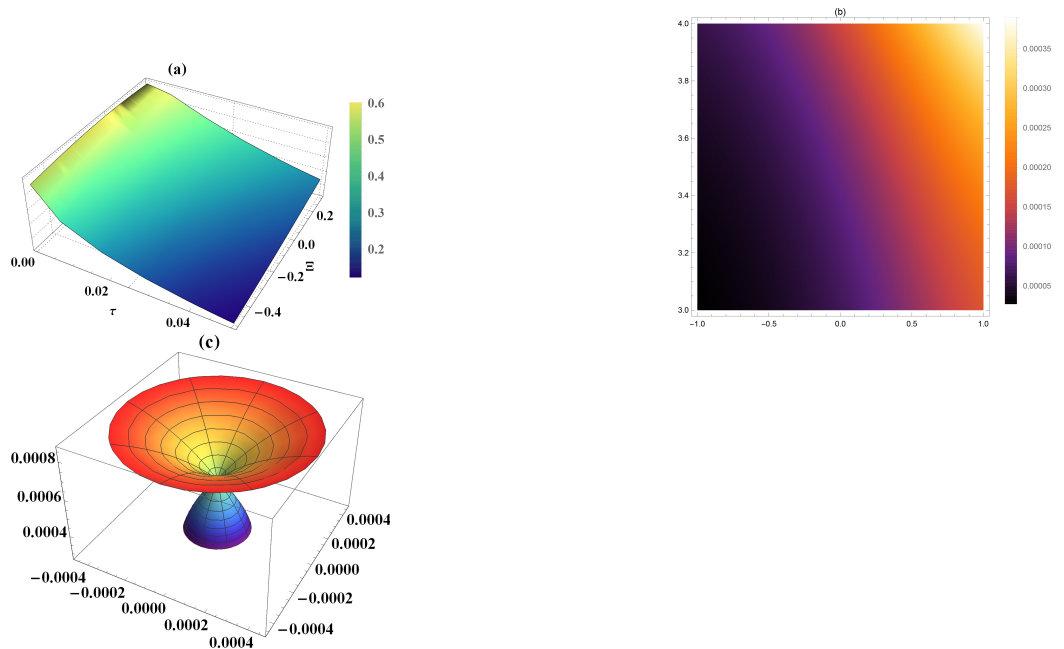


**Figure 3.** Solitary wave solution of Equation (32) in (a) three–dimension, (b) density and (c) spherical plot three–dimensional for  $a = 3$ ,  $\varrho = 0.5$ .

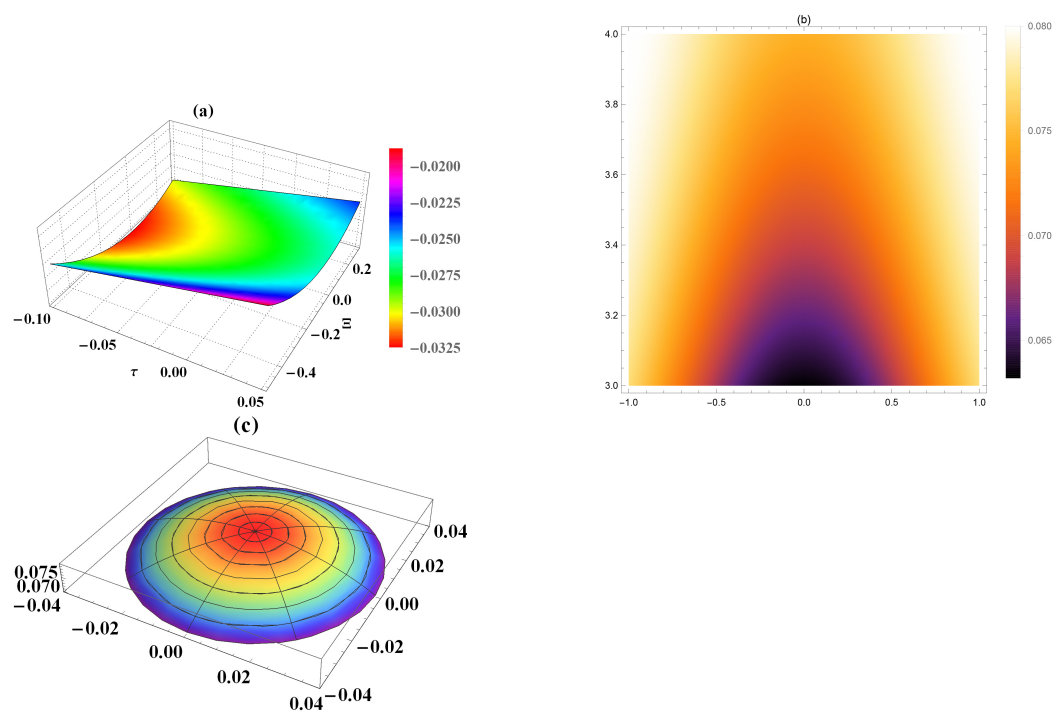


**Figure 4.** Solitary wave solution of Equation (33) in (a) three–dimension, (b) density and (c) spherical plot three–dimensional for  $a = 2$ ,  $\varrho = 0.5$ .

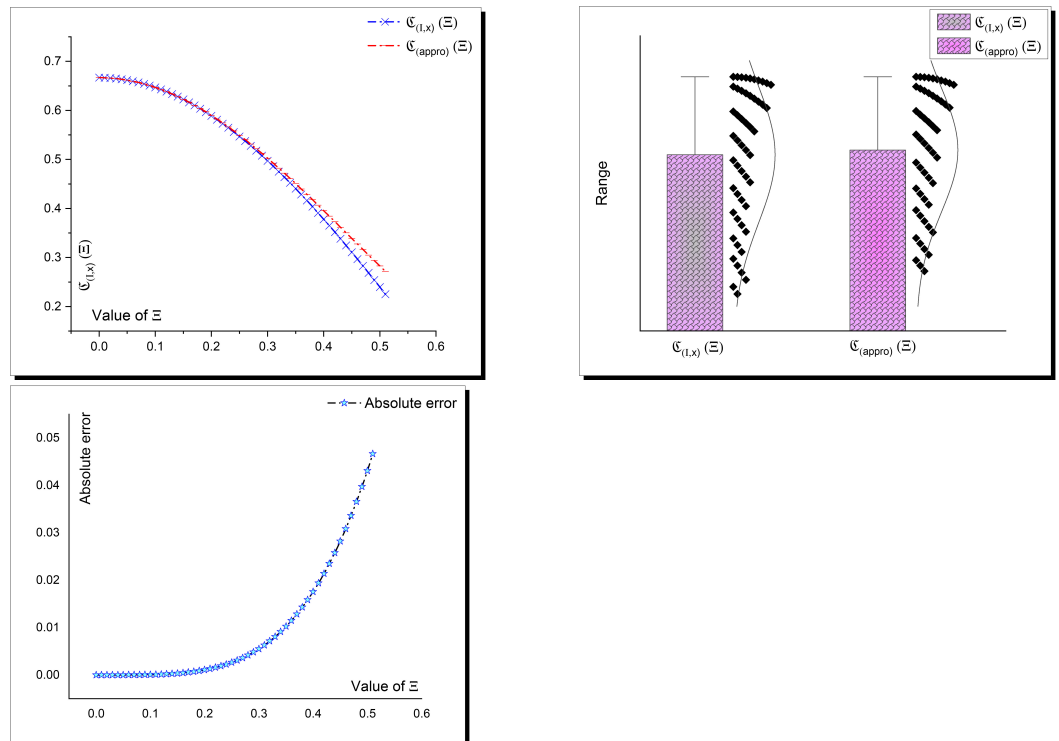


**Figure 5.** Matching between exact and semi–analytical solutions based on Table 1.

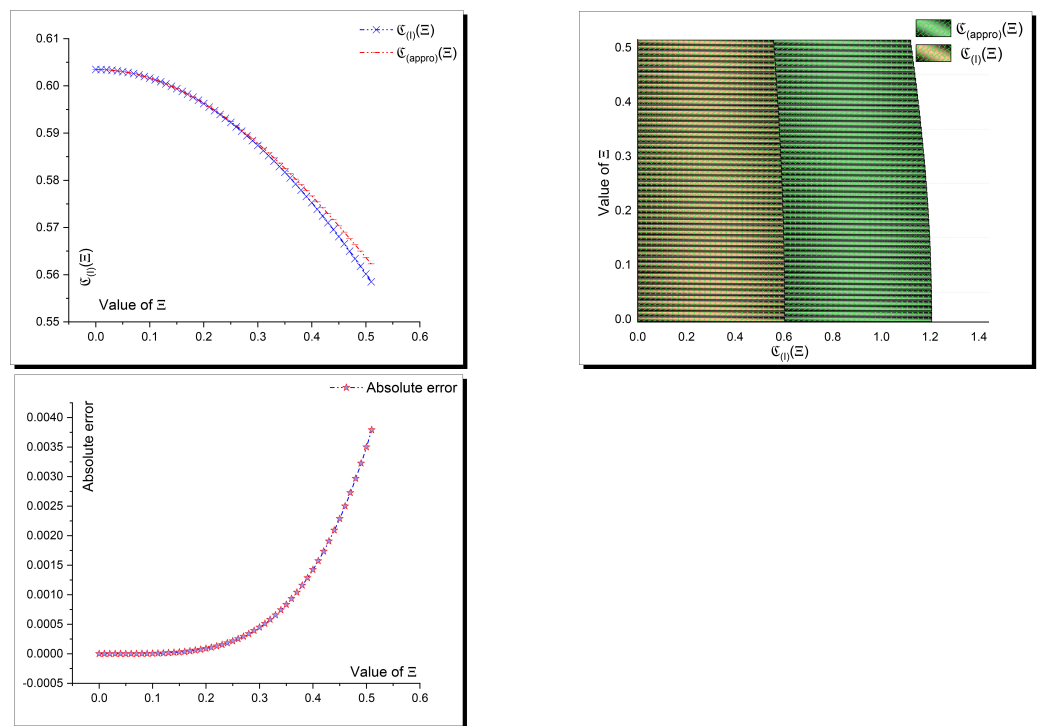


**Figure 6.** Matching between exact and semi-analytical solutions based on Table 2.

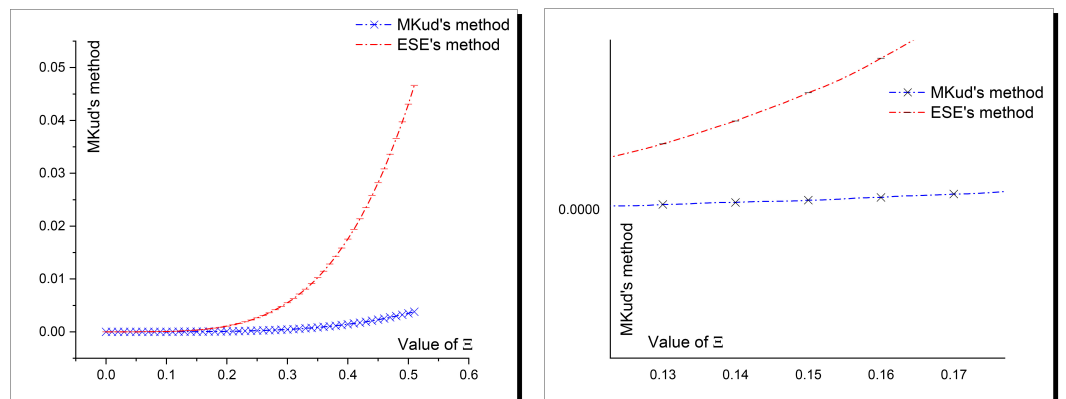


**Figure 7.** MKud method's superiority.

#### 4. Conclusions

This article has successfully implemented two recent analytical schemes (ESE and MKud techniques), and many novel solutions have been obtained for the considered model. The conformable fractional derivative has been employed to convert the fractional system to a system with an integer. The exact solutions have been demonstrated through 3D, density, spherical plot 3D sketches. Moreover, the accuracy of the obtained solutions has been illustrated by calculating the absolute value of error between the exact and semi-analytical methods accepted by the AD method. The novelty of the obtained results in this article has been explained by comparing our results with the previously published research paper.

**Author Contributions:** Conceptualization, C.Y.; methodology, C.Y.; formal analysis, M.M.A.K.; investigation, M.M.A.K.; writing—original draft, C.Y.; writing—review and editing, C.Y.; visualization, M.M.A.K.; supervision, D.L.; data curation, C.Y.; resources, D.L. All authors have read and agreed to the published version of the manuscript.

**Funding:** This paper has been funded by the Research Innovation Program for College Graduates of Jiangsu Province (Grant No.KYCX19–1609).

**Data Availability Statement:** The data that support the findings of this study are available from the corresponding author upon reasonable request.

**Acknowledgments:** The author would like to thank the journal stuff (Editor & Reviewers).

**Conflicts of Interest:** The authors declare no conflict of interest.

## References

1. Abdel-Aty, A.H.; Khater, M.M.; Dutta, H.; Bouslimi, J.; Omri, M. Computational solutions of the HIV-1 infection of CD4+ T-cells fractional mathematical model that causes acquired immunodeficiency syndrome (AIDS) with the effect of antiviral drug therapy. *Chaos Solitons Fractals* **2020**, *139*, 110092. [[CrossRef](#)]
2. Abdel-Aty, A.H.; Khater, M.M.; Attia, R.A.; Abdel-Aty, M.; Eleuch, H. On the new explicit solutions of the fractional nonlinear space-time nuclear model. *Fractals* **2020**, *28*, 2040035. [[CrossRef](#)]
3. Jena, R.; Chakraverty, S.; Yavuz, M. Two-hybrid techniques coupled with an integral transform for Caputo time-fractional Navier-Stokes Equations. *Prog. Fract. Differ. Appl.* **2020**, *6*, 201–213.
4. Abdel-Aty, A.H.; Khater, M.M.; Baleanu, D.; Khalil, E.; Bouslimi, J.; Omri, M. Abundant distinct types of solutions for the nervous biological fractional FitzHugh–Nagumo equation via three different sorts of schemes. *Adv. Differ. Equ.* **2020**, *2020*, 1–17. [[CrossRef](#)]
5. Khater, M.M.; Attia, R.A.; Park, C.; Lu, D. On the numerical investigation of the interaction in plasma between (high & low) frequency of (Langmuir & ion-acoustic) waves. *Results Phys.* **2020**, *18*, 103317.
6. Khater, M.M.; Nofal, T.A.; Abu-Zinadah, H.; Lotayif, M.S.; Lu, D. Novel computational and accurate numerical solutions of the modified Benjamin–Bona–Mahony (BBM) equation arising in the optical illusions field. *Alex. Eng. J.* **2020**, *60*, 1797–1806. [[CrossRef](#)]
7. Yavuz, M.; Yokus, A. Analytical and numerical approaches to nerve impulse model of fractional-order. *Numer. Methods Partial. Differ. Equ.* **2020**, *36*, 1348–1368. [[CrossRef](#)]
8. Khater, M.M.; Attia, R.A.; Mahmoud, E.E.; Abdel-Aty, A.H.; Abualnaja, K.M.; Mohamed, A.B.; Eleuch, H. On the interaction between (low & high) frequency of (ion-acoustic & Langmuir) waves in plasma via some recent computational schemes. *Results Phys.* **2020**, *19*, 103684.
9. Khater, M.M.; Attia, R.A.; Baleanu, D. Abundant new solutions of the transmission of nerve impulses of an excitable system. *Eur. Phys. J. Plus* **2020**, *135*, 1–12. [[CrossRef](#)]
10. Khater, M.M.; Attia, R.A.; Lu, D. Computational and numerical simulations for the nonlinear fractional Kolmogorov–Petrovskii–Piskunov (FKPP) equation. *Phys. Scr.* **2020**, *95*, 055213. [[CrossRef](#)]
11. Yavuz, M.; Sulaiman, T.A.; Usta, F.; Bulut, H. Analysis and numerical computations of the fractional regularized long-wave equation with damping term. *Math. Methods Appl. Sci.* **2020**, *44*, 7538–7555. [[CrossRef](#)]
12. Khater, M.M.; Mohamed, M.S.; Park, C.; Attia, R.A. Effective computational schemes for a mathematical model of relativistic electrons arising in the laser thermonuclear fusion. *Results Phys.* **2020**, *19*, 103701. [[CrossRef](#)]
13. Abdel-Aty, A.H.; Khater, M.M.; Baleanu, D.; Abo-Dahab, S.; Bouslimi, J.; Omri, M. Oblique explicit wave solutions of the fractional biological population (BP) and equal width (EW) models. *Adv. Differ. Equ.* **2020**, *2020*, 1–17. [[CrossRef](#)]
14. Yavuz, M.; Sulaiman, T.A.; Yusuf, A.; Abdeljawad, T. The Schrödinger-KdV equation of fractional order with Mittag-Leffler nonsingular kernel. *Alex. Eng. J.* **2021**, *60*, 2715–2724. [[CrossRef](#)]
15. Khater, M.M.; Lu, D.; Hamed, Y. Computational simulation for the (1+1)-dimensional Ito equation arising quantum mechanics and nonlinear optics. *Results Phys.* **2020**, *19*, 103572. [[CrossRef](#)]
16. Rezazadeh, H.; Souleymanou, A.; Korkmaz, A.; Khater, M.M.; Mukam, S.P.; Kuettche, V.K. New exact solitary waves solutions to the fractional Fokas-Lenells equation via Atangana-Baleanu derivative operator. *Int. J. Mod. Phys. B* **2020**, *34*, 2050309. [[CrossRef](#)]
17. Khater, M.; Chu, Y.M.; Attia, R.A.; Inc, M.; Lu, D. On the Analytical and Numerical Solutions in the Quantum Magnetoplasmas: The Atangana Conformable Derivative (2+1)-ZK Equation with Power-Law Nonlinearity. *Adv. Math. Phys.* **2020**, *2020*, 1–10. [[CrossRef](#)]
18. Attia, R.A.; Alfalqi, S.; Alzaidi, J.; Khater, M.; Lu, D. Computational and Numerical Solutions for-Dimensional Integrable Schwarz–Korteweg–de Vries Equation with Miura Transform. *Complexity* **2020**, *2020*, 2394030. [[CrossRef](#)]
19. Qin, H.; Khater, M.; Attia, R.A.; Lu, D. Approximate Simulations for the Non-linear Long-Short Wave Interaction System. *Front. Phys.* **2020**, *7*, 230. [[CrossRef](#)]
20. Gao, W.; Rezazadeh, H.; Pinar, Z.; Baskonus, H.M.; Sarwar, S.; Yel, G. Novel explicit solutions for the nonlinear Zoomeron equation by using newly extended direct algebraic technique. *Opt. Quantum Electron.* **2020**, *52*, 1–13. [[CrossRef](#)]
21. Korkmaz, A.; Hepson, O.E.; Hosseini, K.; Rezazadeh, H.; Eslami, M. Sine-Gordon expansion method for exact solutions to conformable time fractional equations in RLW-class. *J. King Saud-Univ.-Sci.* **2020**, *32*, 567–574. [[CrossRef](#)]
22. Jajarmi, A.; Yusuf, A.; Baleanu, D.; Inc, M. A new fractional HRSV model and its optimal control: A non-singular operator approach. *Phys. Stat. Mech. Its Appl.* **2020**, *547*, 123860. [[CrossRef](#)]
23. Inc, M.; Korpinar, Z.; Almohsen, B.; Chu, Y.M. Some numerical solutions of local fractional tricomi equation in fractal transonic flow. *Alex. Eng. J.* **2020**, *60*, 1147–1153. [[CrossRef](#)]

24. Wang, K.J.; Wang, G.D. Variational principle and approximate solution for the fractal generalized Benjamin-Bona-Mahony-Burgers Equation in Fluid Mechanics. *Fractals* **2020**. [[CrossRef](#)]
25. Yavuz, M.; Sene, N. Approximate solutions of the model describing fluid flow using generalized  $\rho$ -laplace transform method and heat balance integral method. *Axioms* **2020**, *9*, 123. [[CrossRef](#)]
26. Yavuz, M.; Abdeljawad, T. Nonlinear regularized long-wave models with a new integral transformation applied to the fractional derivative with power and Mittag-Leffler kernel. *Adv. Differ. Equ.* **2020**, *2020*, 1–18. [[CrossRef](#)]
27. Ali, A.T.; Khater, M.M.; Attia, R.A.; Abdel-Aty, A.H.; Lu, D. Abundant numerical and analytical solutions of the generalized formula of Hirota-Satsuma coupled KdV system. *Chaos Solitons Fractals* **2020**, *131*, 109473. [[CrossRef](#)]
28. Zhao, Z.; He, L. M-lump and hybrid solutions of a generalized (2+ 1)-dimensional Hirota-Satsuma-Ito equation. *Appl. Math. Lett.* **2021**, *111*, 106612. [[CrossRef](#)]
29. Zhang, L.D.; Tian, S.F.; Peng, W.Q.; Zhang, T.T.; Yan, X.J. The dynamics of lump, lumpoff and rogue wave solutions of (2+ 1)-dimensional Hirota-Satsuma-Ito equations. *East Asian J. Appl. Math.* **2020**, *10*, 243–255. [[CrossRef](#)]
30. Tala-Tebue, E.; Rezazadeh, H.; Djoufack, Z.I.; Eslam, M.; Kenfack-Jiotsa, A.; Bekir, A. Optical solutions of cold bosonic atoms in a zig-zag optical lattice. *Opt. Quantum Electron.* **2021**, *53*, 1–13. [[CrossRef](#)]
31. Chu, Y.; Shallal, M.A.; Mirhosseini-Alizamini, S.M.; Rezazadeh, H.; Javeed, S.; Baleanu, D. Application of Modified Extended Tanh Technique for Solving Complex Ginzburg–Landau Equation Considering Kerr Law Nonlinearity. *CMC-Comput. Mater. Contin.* **2021**, *66*, 1369–1378. [[CrossRef](#)]
32. da Silva, T.F.; Casarotti, S.N.; de Oliveira, G.L.V.; Penna, A.L.B. The impact of probiotics, prebiotics, and symbiotics on the biochemical, clinical, and immunological markers, as well as on the gut microbiota of obese hosts. *Crit. Rev. Food Sci. Nutr.* **2021**, *61*, 337–355. [[CrossRef](#)] [[PubMed](#)]
33. Osman, M.; Korkmaz, A.; Rezazadeh, H.; Mirzazadeh, M.; Eslami, M.; Zhou, Q. The unified method for conformable time fractional Schroö dinger equation with perturbation terms. *Chin. J. Phys.* **2018**, *56*, 2500–2506. [[CrossRef](#)]
34. Liu, J.G.; Eslami, M.; Rezazadeh, H.; Mirzazadeh, M. Rational solutions and lump solutions to a non-isospectral and generalized variable-coefficient Kadomtsev–Petviashvili equation. *Nonlinear Dyn.* **2019**, *95*, 1027–1033. [[CrossRef](#)]
35. Shen, W.; Ma, Z.; Fei, J.; Zhu, Q. Novel characteristics of lump and lump–soliton interaction solutions to the (2+ 1)-dimensional Alice–Bob Hirota-Satsuma-Ito equation. *Mod. Phys. Lett. B* **2020**, *34*, 2050419. [[CrossRef](#)]